J|A|C|S
ARTICLES
Published on Web 12/06/2006

Expression of a Supramolecular Complex at a Multivalent Interface

Olga Crespo-Biel,† Choon Woo Lim,† Bart Jan Ravoo,† David N. Reinhoudt,† and Jurriaan Huskens*,†,‡

Contribution from the Laboratories for Supramolecular Chemistry & Technology and Molecular Nanofabrication, and Strategic Research Orientation "Nanofabrication", MESA+ Institute for Nanotechnology, University of Twente, P.O. Box 217, 7500 AE, Enschede, The Netherlands

Received May 30, 2006; E-mail: j.huskens@utwente.nl

Abstract: The multivalent binding of a supramolecular complex at a multivalent host surface by combining the orthogonal β-cyclodextrin (CD) host−guest and metal ion−ethylenediamine coordination motifs is described. As a heterotropic, divalent linker, an adamantyl-functionalized ethylenediamine derivative was used. This was complexed with Cu(II) or Ni(II). The binding of the complexes to a CD self-assembled monolayer (SAM) was studied as a function of pH by means of surface plasmon resonance (SPR) spectroscopy. A heterotropic, multivalent binding model at interfaces was used to quantify the multivalent enhancement at the surface. The Cu(II) complex showed divalent binding to the CD surface with an enhancement factor higher than 100 relative to the formation of the corresponding divalent complex in solution. Similar behavior was observed for the Ni(II) system. Although the Ni(II) system could potentially be trivalent, only divalent binding was observed at the CD SAMs, which was confirmed by desorption experiments.

Multivalent interactions involve the simultaneous interaction between multiple (two or more) functionalities on one entity and complementary functionalities on another.[1] Multivalent interactions are involved in a variety of biological processes such as cell signaling, pathogen identification, and inflammatory response.[1,2] Multivalent binding events have unique collective properties that are qualitatively and quantitatively different from the properties displayed by their monovalent constituents. For example, multivalent interactions can achieve higher binding affinities and can afford larger contact areas between surfaces.[3]

For mechanistic studies of multivalent interactions, receptors anchored on a surface offer several advantages over receptors in solution. One of the main advantages is the relative ease of preparation of the building blocks, because a monovalent receptor becomes multivalent upon immobilization. A second important advantage is that the binding strength is enhanced in multivalent complexes compared to the corresponding monovalent parent. This effect can commonly be ascribed to an effective concentration (C_{eff}) term. It represents a probability of interaction between two reactive or complementary interlinked entities and symbolizes a "physically real" concentration of one of the reacting or interacting functionalities as experienced by its complementary counterpart.[4,5] To this aim, different template substrates have been synthesized to serve as model systems for cell membranes, such as self-assembled monolayers (SAMs),[6] nanoparticles,[7] and vesicles.[8]

The development of functional surfaces and supramolecular structures built upon them by the assembly of molecular building blocks is an important issue in nanotechnology.[9] Furthermore, supramolecular interactions have been employed for the immobilization of molecules at surfaces, achieving characteristic features such as high specificity, tunable affinity, and reversibility of immobilization.[10] The use of multiple, intrinsically weak interactions can lead to complexes that are thermodynamically or kinetically stable, where the overall strength can be

† Laboratories for Supramolecular Chemistry & Technology and Molecular Nanofabrication.

‡ Strategic Research Orientation "Nanofabrication".

(1) Sigal, G. B.; Mammen, M.; Dahmann, G.; Whitesides, G. M. *J. Am. Chem. Soc.* **1996**, *118*, 3789−3800.
(2) Spaltenstein, A.; Whitesides, G. M. *J. Am. Chem. Soc.* **1991**, *113*, 686−687.
(3) (a) Mammen, M.; Choi, S. K.; Whitesides, G. M. *Angew. Chem., Int. Ed.* **1998**, *37*, 2755−2794. (b) Lundquist, J. J.; Toone, E. J. *Chem. Rev.* **2002**, *102*, 555−578. (c) Varki, A. *Glycobiology* **1993**, *3*, 97−130.
(4) Mulder, A.; Auletta, T.; Sartori, A.; Del Ciotto, S.; Casnati, A.; Ungaro, R.; Huskens, J.; Reinhoudt, D. N. *J. Am. Chem. Soc.* **2004**, *126*, 6627−6636.
(5) Huskens, J.; Mulder, A.; Auletta, T.; Nijhuis, C. A.; Ludden, M. J. W.; Reinhoudt, D. N. *J. Am. Chem. Soc.* **2004**, *126*, 6784−6797.
(6) (a) Mann, D. A.; Kanai, M.; Maly, D. J.; Kiessling, L. L. *J. Am. Chem. Soc.* **1998**, *120*, 10575−10582. (b) Rao, J. H.; Yan, L.; Xu, B.; Whitesides, G. M. *J. Am. Chem. Soc.* **1999**, *121*, 2629−2630. (c) Metallo, S. J.; Kane, R. S.; Holmlin, R. E.; Whitesides, G. M. *J. Am. Chem. Soc.* **2003**, *125*, 4534−4540. (d) Smith, E. A.; Thomas, W. D.; Kiessling, L. L.; Corn, R. M. *J. Am. Chem. Soc.* **2003**, *125*, 6140−6148. (e) Crespo-Biel, O.; Péter, M.; Bruinink, C. M.; Ravoo, B. J.; Reinhoudt, D. N.; Huskens, J. *Chem. Eur. J.* **2005**, *11*, 2426−2432. (f) Nijhuis, C. A.; Yu, F.; Knoll, W.; Huskens, J.; Reinhoudt, D. N. *Langmuir* **2005**, *21*, 7866−7876.
(7) (a) Fantuzzi, G.; Pengo, P.; Gomila, R.; Ballester, P.; Hunter, C. A.; Pasquato, L.; Scrimin, P. *Chem. Commun.* **2003**, 1004−1005. (b) Barrientos, A. G.; De La Fuente, J. M.; Rojas, T. C.; Fernández, A.; Penadés, S. *Chem. Eur. J.* **2003**, *9*, 1909−1921. (c) Lin, C. C.; Yeh, Y. C.; Yang, C. Y.; Chen, G. F.; Chen, Y. C.; Wu, Y. C.; Chen, C. C. *Chem. Commun.* **2003**, 2920−2921.
(8) (a) Thibault, R. J.; Galow, T. H.; Turnberg, E. J.; Gray, M.; Hotchkiss, P. J.; Rotello, V. M. *J. Am. Chem. Soc.* **2002**, *124*, 15249−15254. (b) Lim, C. W.; Ravoo, B. J.; Reinhoudt, D. N. *Chem. Commun.* **2005**, 5627−5629.
(9) Whitesides, G. M. *Small* **2005**, *1*, 172−179.

10.1021/ja0637705 CCC: $33.50

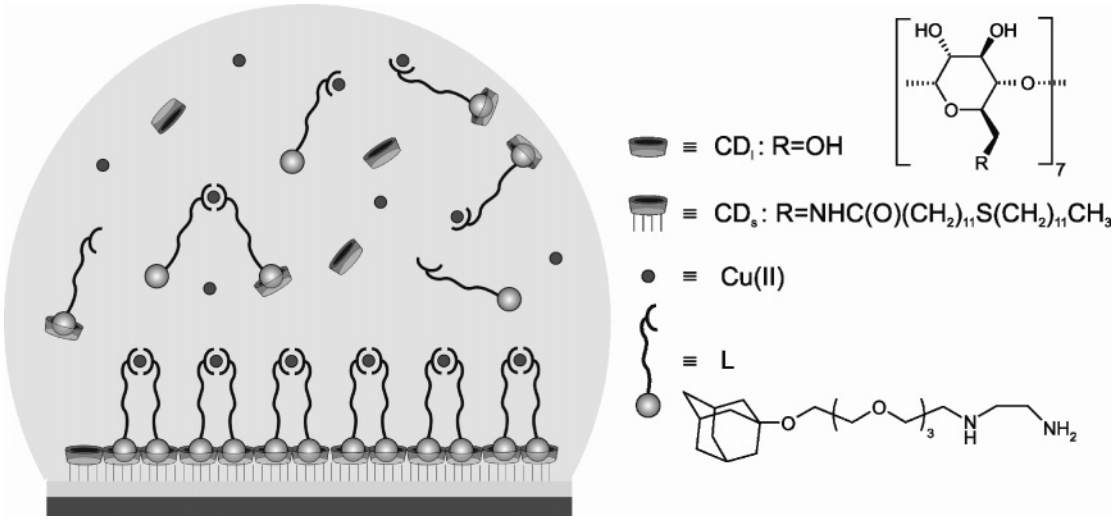

Figure 1. Schematic illustration of the multivalent enhancement concept at CD SAMs induced by the high effective CD concentration (C_{eff}) at the aqueous interface and guest and host compounds used in this study.

fine-tuned by controlling the number of interactions and the strength of the intrinsic interaction.[5]

Metal−ligand interactions have already been successfully used to generate complex molecular architectures with specific topology, high stability, and original properties.[11] Special interest has been focused on the *N*-nitrilotriacetic acid (NTA)-histidine-tag (His_6-tag) chelator system. This approach utilizes the NTA chelator to coordinate divalent metal cations (Cu^{2+}, Ni^{2+}, Zn^{2+}, Co^{2+}) leaving coordination sites of the chelator−metal complex free for the ligation of the His_6-tag. The group of Tampé has used NTA-functionalized lipids[12] and SAMs[13] to immobilize proteins through multivalent interactions. Evidence for multivalent interactions between the His_6-tag and the NTA groups was found in experiments involving immobilization of His_6-tagged proteins on chelating lipid membranes with chelators at different surface concentrations.[12a] In a similar approach, Doyle et al. studied the cooperative binding of Cu^{2+} ions to a membrane-bound synthetic receptor, with a dansyl-ethylenediamine conjugate as the head group and cholesterol as the membrane anchor.[14] This model system allowed to quantify the membrane environment and therefore to investigate the relationship between receptor concentration and the cooperativity of multicomponent assembly processes at the membrane surface.

Heterotropic, orthogonal recognition motifs are intermolecular interactions that operate independently of each other so that no crossover or interference occurs.[15,16] They can lead to higher stoichiometries, better specificities, and more complex architectures than when only one single interaction motif is employed. Supramolecular chemistry has benefited greatly from the simultaneous binding of several orthogonal recognition motifs for the construction of elaborate multicomponent superarchitectures.[16,17] The ultimate example of this is DNA for which every pair of matching single strands is orthogonal to other pairs. This approach has been used to obtain DNA nanostructures.[18]

Here, we report the multivalent binding of a supramolecular complex at a multivalent host surface by combining the orthogonal β-cyclodextrin (CD) host−guest and metal ion-ethylenediamine (M-en) coordination motifs. The system employs a heterotropic divalent linker, with a CD-complexing adamantyl (Ad) group on one end and an M(II)-complexing en unit on the other. This allows the linker to bind to CD in solution as well as to CD immobilized at self-assembled monolayers (SAMs).[19] The binding of Ad guests at such SAMs is fully comparable to binding to CD in solution.[20] These CD SAMs allow a quantitative understanding of (homotropic) multivalent binding at interfaces.[4,5] The C_{eff} of CD hosts at such a SAM is much higher than in solution and less dependent on linker length. The key idea, targeted in the current study, is therefore to investigate whether this high C_{eff} at interfaces can be employed to enhance the presence of multivalent complexes at such interfaces relative to the solution which contains the elementary building blocks.

Results and Discussion

The potential surface enhancement effect at CD SAMs by a multivalent receptor surface is illustrated in Figure 1. Multivalent

(10) (a) Sanyal, A.; Norsten, T. B.; Uzun, O.; Rotello, V. M. *Langmuir* **2004**, *20*, 5958−5964. (b) Park, J. S.; Lee, G. S.; Lee, Y. J.; Park, Y. S.; Yoon, K. B. *J. Am. Chem. Soc.* **2002**, *124*, 13366−13367. (c) Chen, Y. F.; Banerjee, I. A.; Yu, L.; Djalali, R.; Matsui, H. *Langmuir* **2004**, *20*, 8409−8413. (d) Huskens, J.; Deij, M. A.; Reinhoudt, D. N. *Angew. Chem., Int. Ed.* **2002**, *41*, 4467−4471. (e) Fragoso, A.; Caballero, J.; Almirall, E.; Villalonga, R.; Cao, R. *Langmuir* **2002**, *18*, 5051−5054. (f) Zhang, S.; Palkar, A.; Fragoso, A.; Prados, P.; De Mendoza, J.; Echegoyen, L. *Chem. Mater.* **2005**, *17*, 2063−2068.
(11) (a) Holliday, B. J.; Mirkin, C. A. *Angew. Chem., Int. Ed.* **2001**, *40*, 2022−2043. (b) Cotton, F. A.; Lin, C.; Murillo, C. A. *Proc. Natl. Acad. Sci. U.S.A.* **2002**, *99*, 4810−4813.
(12) (a) Dorn, I. T.; Eschrich, R.; Seemuller, E.; Guckenberger, R.; Tampé, R. *J. Mol. Biol.* **1999**, *288*, 1027−1036. (b) Radler, U.; Mack, J.; Persike, N.; Jung, G.; Tampé, R. *Biophys. J.* **2000**, *79*, 3144−3152. (c) Thess, A.; Hutschenreiter, S.; Hofmann, M.; Tampé, R.; Baumeister, W.; Guckenberger, R. *J. Biol. Chem.* **2002**, *277*, 36321−36328.
(13) (a) Gamsjaeger, R.; Wimmer, B.; Kahr, H.; Tinazli, A.; Picuric, S.; Lata, S.; Tampé, R.; Maulet, Y.; Gruber, H. J.; Hinterdorfer, P.; Romanin, C. *Langmuir* **2004**, *20*, 5885−5890. (b) Tinazli, A.; Tang, J. L.; Valiokas, R.; Picuric, S.; Lata, S.; Piehler, J.; Liedberg, B.; Tampé, R. *Chem. Eur. J.* **2005**, *11*, 5249−5259.
(14) Doyle, E. L.; Hunter, C. A.; Phillips, H. C.; Webb, S. J.; Williams, N. H. *J. Am. Chem. Soc.* **2003**, *125*, 4593−4599.
(15) Fyfe, M. C. T.; Stoddart, J. F. *Coord. Chem. Rev.* **1999**, *183*, 139−155.
(16) Hofmeier, H.; Schubert, U. S. *Chem. Commun.* **2005**, 2423−2432.
(17) Some examples can be found: (a) Thalladi, V. R.; Goud, B. S.; Hoy, V. J.; Allen, F. H.; Howard, J. A. K.; Desiraju, G. R. *Chem. Comm.* **1996**, 401−402. (b) Funeriu, D. P.; Lehn, J. M.; Baum, G.; Fenske, D. *Chem. Eur. J.* **1997**, *3*, 99−104.
(18) (a) Rosi, N. L.; Mirkin, C. A. *Chem. Rev.* **2005**, *105*, 1547−1562. (b) Samori, B.; Zuccheri, G. *Angew. Chem., Int. Ed.* **2005**, *44*, 1166−1181.
(19) Beulen, M. W. J.; Bügler, J.; De Jong, M. R.; Lammerink, B.; Huskens, J.; Schönherr, H.; Vancso, G. J.; Boukamp, B. A.; Wieder, H.; Offenhäuser, A.; Knoll, W.; Van Veggel, F. C. J. M.; Reinhoudt, D. N. *Chem. Eur. J.* **2000**, *6*, 1176−1183.
(20) De Jong, M. R.; Huskens, J.; Reinhoudt, D. N. *Chem. Eur. J.* **2001**, *7*, 4164−4170.

Scheme 1. Equilibria for All Solution Species of L, in the Absence and Presence of M(II) and CD_l (Charges Are Omitted for Clarity)

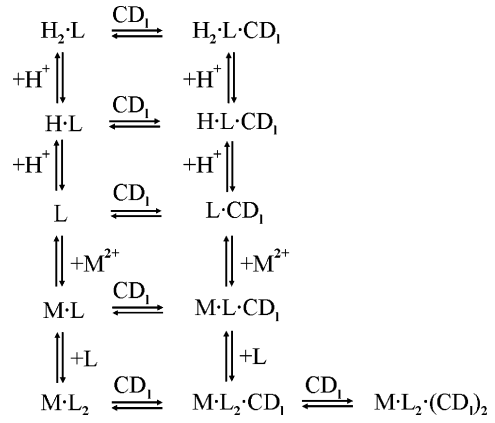

building blocks consisting of a single binding motif (CD SAMs and M^{2+} ions) and a divalent linker with complementary units of both motifs were employed. The two interaction motifs (CD-Ad and M-en) are considered to be orthogonal, but this is studied in detail below. As the metal−ligand coordination motif, the Cu(II)-en and Ni(II)-en interaction pairs were used with Cu(II) as a divalent building block and Ni(II) as a (potentially) trivalent one.

As a heterotropic, divalent linker, the Ad-functionalized en derivative ligand L was used (Figure 1). Linker L was designed (1) to interact with CD (in solution and at CD SAMs) through the Ad moiety, (2) to coordinate to M(II) through the en moiety, and (3) to provide a sufficiently long linker to allow divalent host−guest binding to the CD SAMs when two ligands are coordinated to the M(II) center. CD SAMs on gold[20] (CD_s, host) were chosen as the monotropic multivalent display for the CD host−guest interaction motif. This type of host with long alkyl chains is especially suitable for this study because it forms densely packed, well-ordered SAMs.[21] These CD SAMs allow a fundamental understanding of multivalent binding at the surface, which has been correlated previously, to binding studies in solution.[4] The hexagonal packing of these SAMs has been observed with high-resolution AFM.[22] The center-to-center distance between the CDs is approximately 2.1 nm.

The basicity of the amino groups makes the complexation to metal cations pH dependent. In principle, it is assumed that all guest species present—protonated, unprotonated, or metal-complexed—are able to bind CD. The oligo(ethylene glycol) chain is used to provide enough length and flexibility for binding the CD SAM in a multivalent fashion, while retaining water solubility and preventing nonspecific interactions. All solution species of L, resulting from protonation, metal complexation, and CD_l complexation, are given in Scheme 1.[23] When full orthogonality is assumed, all intrinsic stability constants for complexation by cyclodextrin in solution, CD_l, of any species of L are equal, but this is to be verified experimentally (see below).

At a CD SAM surface, all species containing one molecule of L will behave as monovalent guests, binding a single surface

Scheme 2. Equilibria for Solution and Surface Species of ML_2

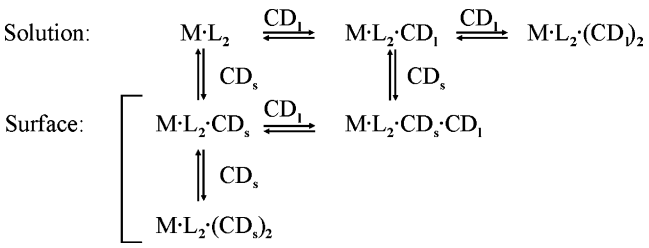

CD in a similar manner as in solution. In contrast, the divalent ML_2 is expected to show the equilibria give in Scheme 2. This behavior is expected for M═Cu(II), while Ni(II) can potentially be trivalent, that is, give NiL_3 complexes. From previous studies, it is known that the formation of $M{\cdot}L_2{\cdot}(CD_s)_2$ is governed by an effective concentration (C_{eff}) term, which is the driving force for the preferential formation of such multivalent species at the multivalent CD SAMs.[4,5]

The first metal ion chosen for this study was Cu(II) which forms divalent ($Cu{\cdot}en_2$) complexes with a square-planar geometry.[24] The cis- and trans- configurations are likely to behave similarly in our studies since (1) the total lengths of the linkers between the Ad groups (2.9 and 3.2 nm) are larger than the lattice periodicity of the CD SAMs (2.1 nm)[22] and (2) differences in length and flexibility of the oligo(ethylene glycol) chain are not expected to lead to significant differences in C_{eff}.[4,5] The metal complex was prepared by mixing a solution of L and $CuCl_2$ in a 2:1 molar ratio.

Because L is a monosubstituted en derivative, we used protonation[25] and metal-complex formation[26] constants of *N*-*n*-butylethylenediamine to calculate speciations in solution (Figure 2), while noting that these constants do not vary significantly within the class of monosubstituted en derivatives.[27] As mentioned above, the basicity of the amino groups makes the complexation to metal cations pH dependent. This leads to an expected pH dependence of the speciation of L in the absence and presence of Cu(II) as shown in Figure 2, left and right, respectively. When looking at the valencies of the species regarding binding to CD SAMs, that is, the number of Ad groups, all species in the absence of Cu(II) are obviously monovalent. When Cu(II) is present in the solution at a 1:2 M:L ratio, the only divalent species, CuL_2, starts forming only at pH 6 and is the major species at pH > 6.8 (Figure 2, right).

To verify the orthogonality of the Cu-en CD-Ad binding motifs, binding studies of L, with or without Cu(II) at various pH's, with CD_l were performed in aqueous solution using isothermal titration calorimetry (ITC). Figure 3 depicts the exothermic heat profiles obtained from the calorimetric titration of L (left) and a 1:2 Cu^{2+}:L mixture (right) with CD_l at pH 7.

In the absence of Cu(II), average thermodynamic parameters ($K_{i,l} = (6.0 \pm 0.4) \times 10^4\ M^{-1}$ and $\Delta H° = -5.7$ kcal/mol) were within experimental error identical at various pH values (pH 2−9) and did not differ significantly from known CD-Ad stability constants.[28] In the presence of Cu(II) (Cu:L = 1:2, pH 7−9), the experimental curve for the complexation of L with CD_l was fitted to a 2:1 binding model considering the two Ad

(21) Ulman, A. *An Introduction to Ultrathin Organic Films: From Langmuir-Blodgett to Self-Assembly*; Academic Press: Boston, MA, 1991.
(22) Schönherr, H.; Beulen, M. W. J.; Bügler, J.; Huskens, J.; Van Veggel, F. C. J. M.; Reinhoudt, D. N.; Vancso, G. J. *J. Am. Chem. Soc.* **2000**, *122*, 4963−4967.
(23) Charges are omitted for clarity.
(24) Mellor, D. P. *Chem. Rev.* **1943**, *33*, 137−183.
(25) Basolo, F.; Murmann, R. K. *J. Am. Chem. Soc.* **1952**, *74*, 2373−2374.
(26) Basolo, F.; Murmann, R. K. *J. Am. Chem. Soc.* **1952**, *74*, 5239−5246.
(27) Sillen, L. G.; Martell, A. E. *Stability Constants of Metal-Ion Complexes. Section 2: Organic Ligands*; The Chemical Society: London, 1964.
(28) Rekharsky, M. V.; Inoue, Y. *Chem. Rev.* **1998**, *98*, 1875−1917.

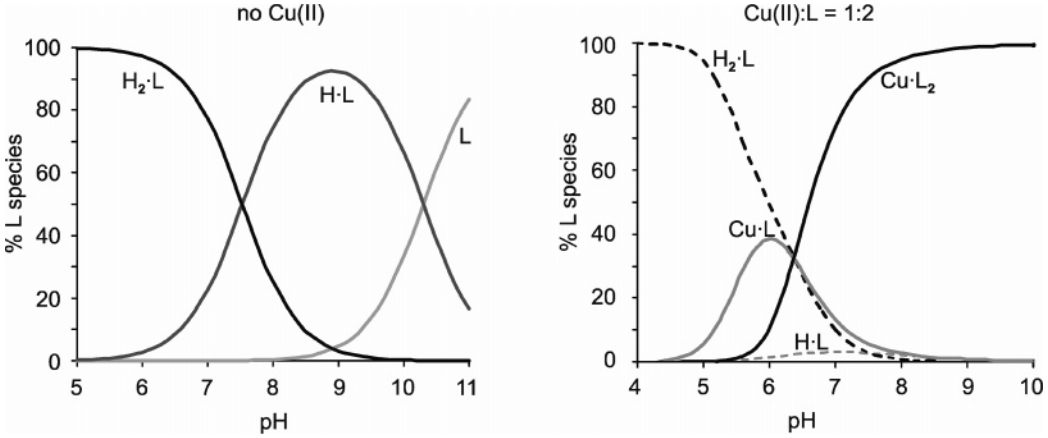

Figure 2. Calculated speciation of L present in solution as a function of pH in the absence (left) and presence (right) of Cu(II) (total concentration of L: 1 mM; with Cu(II): total concentration of Cu(II): 0.5 mM). In the presence of Cu(II) (right), solid lines represent Cu(II) complexes and dashed lines represent species without Cu(II).

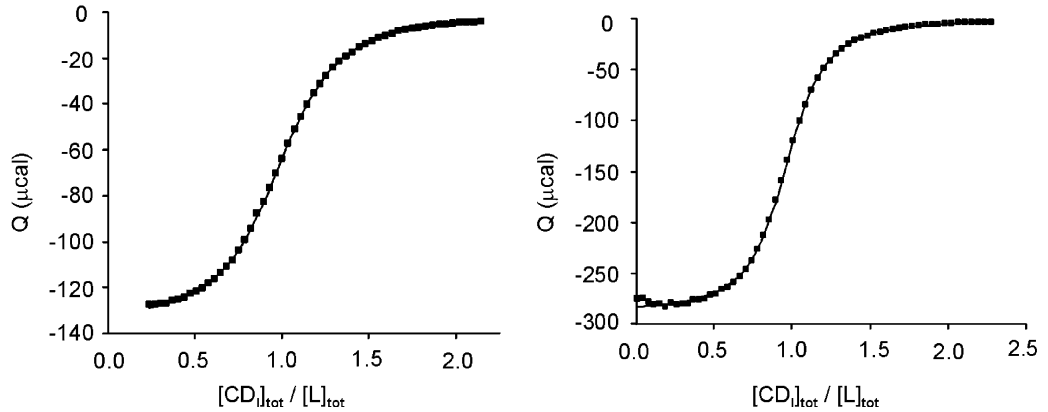

Figure 3. Heat involved per injection plotted against the molar ratio (markers) and fits (solid lines) for the calorimetric titrations of L (5 mM) to CD_l (0.5 mM) (left) and of CD_l (10 mM) to $CuCl_2$ (0.5 mM) and L (1 mM) (right) in water (pH = 7) at 298 K.

Table 1. Thermodynamic Parameters of the Complexation of CD_l with L in the Presence and Absence of Cu(II), as Determined by ITC at 298 K

guest	pH	stoichiometry (host–guest)	$K_{i,l}$ (M^{-1})	$\Delta H°$ (kcal·mol^{-1})	$T\Delta S°$ (kcal·mol^{-1})
L	2	1:1	6.1×10^4	−6.0	−0.2
	7	1:1	6.4×10^4	−5.9	−0.1
	9	1:1	5.5×10^4	−5.2	0.6
Cu(II):L (1:2)	7	1:2	6.2×10^4	−5.7	1.2
	9	1:2	9.6×10^4	−5.2	2.0

groups as independent binding sites. The average intrinsic binding constant ($K_{i,l} = 7.9 \times 10^4$ M^{-1}) and the enthalpy of binding ($\Delta H° = -5.4$ kcal mol^{-1}) are very similar to the thermodynamic parameters obtained for the complexation of L with CD_l in the absence of Cu(II). The fact that the CD-complexing stability constants of the various protonated and Cu(II)-complexed forms are all very similar indicates that the CD-Ad and M-en interactions can be regarded as orthogonal. The thermodynamic parameters obtained at different pH's are listed in Table 1.

The binding of L (in the presence and absence of 0.5 equiv of Cu(II)) at a CD SAM (CD_s) was studied as a function of pH by means of surface plasmon resonance (SPR) spectroscopy. SPR titrations were performed in the presence of 1 mM buffer, and of 1 mM CD_l, to ensure thermodynamic equilibrium. Addition of L resulted in an increase of reflectivity, indicative of adsorption of L at the host SAM. After reaching equilibrium, rinsing of the cell with buffer and 10 mM CD_l led to restoration of the original SPR signal, which indicates the complete desorption of L from the surface. All experiments led, within experimental error, to the same I_{max}, which suggests that similar surface coverages were reached and that neither protonation nor Cu(II) complexation cause response differences. For easy comparison, therefore, all titration curves are merged in a normalized graph (Figure 4). Titrations performed with L in the presence of Cu(II) at pH 6 on 11-mercapto-1-undecanol reference SAMs (not shown) only exhibited a small refractive index effect on the SPR signal, which could be instantaneously restored by rinsing the SAMs with the buffer solution at 1 mM CD_l. Therefore, the adsorption of L to the CD SAM is attributed to specific host−guest interactions.

The Langmuir binding constant ($K_{Langmuir} = 2.3 \times 10^6$ M^{-1}), obtained for a fit of the SPR curve at pH 9, was more than an order of magnitude higher than for the monovalent binding of L in solution. This indicates divalent binding at pH 9, in line with the CuL_2 species being dominant in solution at this pH (Figure 2, right). At pH 5, $K_{Langmuir}$ (1.4×10^5 M^{-1}) is equal to $K_{Langmuir}$ (1.3×10^5 M^{-1}) obtained for the binding of L to the CD SAM in the absence of Cu(II). Again, this can be explained from the speciation diagram in solution (Figure 2, right): at pH 5, the major ligand species is the monovalent H_2L, and thus monovalent binding is expected. In contrast, fitting the data for pH 6 gave an intermediate value (2.7×10^5 M^{-1}) suggesting both divalent and monovalent binding, whereas the expected

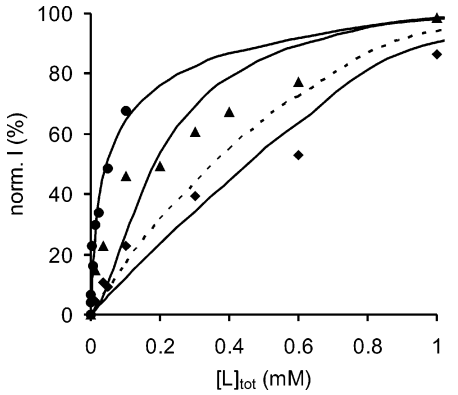

Figure 4. The normalized SPR data points (◆ pH 5; ▲ pH 6; ● pH 9) and the corresponding fits (solid lines) according to the multivalency model (see below) for the different titrations of L in the presence of Cu(II) (Cu(II):L = 1:2) to the CD SAMs. The dashed line corresponds to the normalized fit of the adsorption of L in the absence of Cu(II) to the CD SAM at pH 6.

Table 2. Stability Constants $K_{Langmuir}$ and $K_{i,s}$ of the Complexation of L in the Presence and Absence of Cu(II) to a CD SAM, as Fitted to a Langmuir Isotherm and to the Heterotropic Multivalency Model, Respectively

guest	pH	$K_{Langmuir}$ (M^{-1})	$K_{i,s}$ (M^{-1})	I_{max}
L	6	1.3×10^5		0.76
Cu(II):L (1:2)	5	1.4×10^5	8.7×10^4	0.68
	6	2.7×10^5	7.8×10^4	0.63
	9	2.3×10^6	2.1×10^4	0.72

dominant valency in solution (mixture of H_2L and CuL, see Figure 2, right) is clearly monovalent. The thermodynamic parameters obtained by the Langmuir model at different pH's are listed in Table 2.

For a better quantitative understanding, the SPR titration curves were also fitted to an extended version of the multivalency model[5] in which the divalent binding of CuL_2 to the CD surface is represented as two sequential binding events, using the effective concentration (C_{eff}) concept to describe the intramolecular step.[4,29] The heterotropic divalent model at interfaces is given for the divalent binding of a heterotropic supramolecular complex at a multivalent host surface by combining the orthogonal CD host−guest and metal ion-en coordination interaction motifs. Since full orthogonality has been previously shown, all intrinsic stability constants for CD_l or CD_s complexation of any species of L are equal.

Since all measurements are done at a constant and known pH, the ratios between the protonated forms are fixed and determined by the protonation constants. Their equilibria with CD_l and CD_s do not shift these ratios since the binding constants of the protonated forms are identical (full orthogonality). Therefore, the concentration of free, uncomplexed L [L_f] is defined as

$$[L]_f = [L] + [H{\cdot}L] + [H_2{\cdot}L] \quad (1)$$

while the CD-complexed species (for both CD_l and CD_s) are given by

$$[L_f{\cdot}CD] = [L{\cdot}CD] + [H{\cdot}L{\cdot}CD] + [H_2{\cdot}L{\cdot}CD] \quad (2)$$

Thus, the (simplified) mass balances for L, M(II), CD_l, and CD_s are given by

$$[L]_{tot} = [L_f] + [M{\cdot}L] + 2[M{\cdot}L_2] + [L_f{\cdot}CD_l] + [M{\cdot}L{\cdot}CD_l] + 2[M{\cdot}L_2{\cdot}CD_l] + 2[M{\cdot}L_2{\cdot}(CD_l)_2] + [L_f{\cdot}CD_s] + [M{\cdot}L{\cdot}CD_s] + 2[M{\cdot}L_2{\cdot}CD_s] + 2[M{\cdot}L_2{\cdot}CD_s{\cdot}CD_l] + 2[M{\cdot}L_2{\cdot}(CD_s)_2] \quad (3)$$

$$[M]_{tot} = [M] + [M{\cdot}L] + [M{\cdot}L_2] + [M{\cdot}L{\cdot}CD_l] + [M{\cdot}L_2{\cdot}CD_l] + [M{\cdot}L_2{\cdot}(CD_l)_2] + [M{\cdot}L{\cdot}CD_s]\,[M{\cdot}L_2{\cdot}CD_s] + [M{\cdot}L_2{\cdot}CD_s{\cdot}CD_l] + [M{\cdot}L_2{\cdot}(CD_s)_2] \quad (4)$$

$$[CD_l]_{tot} = [CD_l] + [L_f{\cdot}CD_l] + [M{\cdot}L{\cdot}CD_l] + [M{\cdot}L_2{\cdot}CD_l] + 2[M{\cdot}L_2{\cdot}(CD_l)_2] + [M{\cdot}L_2{\cdot}CD_s{\cdot}CD_l] \quad (5)$$

$$[CD_s]_{tot} = [CD_s] + [L_f{\cdot}CD_s] + [M{\cdot}L{\cdot}CD_s] + [M{\cdot}L_2{\cdot}CD_s] + [M{\cdot}L_2{\cdot}CD_s{\cdot}CD_l] + 2[M{\cdot}L_2{\cdot}(CD_s)_2] \quad (6)$$

The protonation and metal complexation constants of L are given by

$$K_{HL} = \frac{[H{\cdot}L]}{[H][L]} \quad (7)$$

$$K_{H2L} = \frac{[H_2{\cdot}L]}{[H{\cdot}L][H]} \quad (8)$$

$$K_{ML} = \frac{[M{\cdot}L]}{[M][L]} \quad (9)$$

$$K_{ML2} = \frac{[M{\cdot}L_2]}{[M{\cdot}L][L]} \quad (10)$$

For all monovalent species X (X = L, HL, H_2L, ML), the stability constants for CD complexation are given by

$$K_{i,l} = \frac{[X{\cdot}CD_l]}{[X][CD_l]} \quad (11)$$

$$K_{i,s} = \frac{[X{\cdot}CD_s]}{[X][CD_s]} \quad (12)$$

Species involving CD_s are expressed in volume concentrations employing the total sample volume.[4,5]

For the divalent ML_2, binding to CD_l involves statistical factors arising from the probabilities for binding relative to the monovalent species. Similarly, the first binding constant of ML_2 with the CD SAM is defined by

$$\frac{[M{\cdot}L_2{\cdot}CD_s]}{[M{\cdot}L_2][CD_s]} = 2K_{i,s} \quad (13)$$

The second intramolecular binding event at the surface, that is, the formation of $ML(CD_s)_2$, is accompanied by an effective concentration term.[4,5]

$$\frac{[M{\cdot}L_2{\cdot}(CD_s)_2]}{[M{\cdot}L_2{\cdot}CD_s][CD_s]} = \frac{1}{2} C_{eff} K_{i,s} \quad (14)$$

(29) Whether the intramolecular step is assumed to occur for binding of CuL_2 to a CD SAM or for binding of Cu(II) to surface-adsorbed L is irrelevant for this equilibrium analysis.

The effective concentration, C_{eff}, is given by multiplying the maximum effective concentration, $C_{eff,max}$, which is the number of accessible host sites in the probing volume,[4,5] with the fraction of the free host sites at the surface:

$$C_{eff} = C_{eff,max} \frac{[CD_s]}{[CD_s]_{tot}} \quad (15)$$

Substitution of the equilibrium constant definitions into the mass balances for $[L]_{tot}$, $[M]_{tot}$, $[CD_l]_{tot}$, and $[CD_s]_{tot}$ provides a set of numerically solvable species with [L], [M], $[CD_l]$, and $[CD_s]$ as the variables. Starting from an initial estimate for $K_{i,s}$, using fixed values for $C_{eff,max}$ and all other stability constants, this set of equations is solved numerically using a Simplex algorithm in a spreadsheet approach.[30] When fitting SPR data, $K_{i,s}$ is optimized in a least-squares optimization routine, assuming that the SPR response (I) is linearly dependent on the total amount of L adsorbed to the CD SAM regardless of the type of species. The maximum intensity, I_{max}, is then optimized as an independent fitting parameter as well.

For calculating the surface enhancement factor, *EF* (see below), the ratios of divalent to monovalent species, both in solution and at the surface, are compared. In solution, the total concentration of monovalent species, $[L]_{mono}$, is given by

$$[L]_{l,mono} = [L_f] + [M{\cdot}L] + [L_f{\cdot}CD_l] + [M{\cdot}L{\cdot}CD_l] \quad (16)$$

whereas the total concentration of divalent species, $[L]_{l,div}$, is given by

$$[L]_{l,div} = [M{\cdot}L_2] + 2[M{\cdot}L_2{\cdot}CD_l] + 2[M{\cdot}L_2{\cdot}(CD_l)_2] \quad (17)$$

At the surface, the corresponding concentrations, $[L]_{s,mono}$ and $[L]_{s,div}$, are given by

$$[L]_{s,mono} = [L_f{\cdot}CD_s] + [M{\cdot}L{\cdot}CD_s] + 2[M{\cdot}L_2{\cdot}CD_s] + 2[M{\cdot}L_2{\cdot}CD_s{\cdot}CD_l] \quad (18)$$

$$[L]_{s,div} = 2[M{\cdot}L_2{\cdot}(CD_s)_2] \quad (19)$$

The values obtained for the intrinsic stability constants for binding to CD_s, $K_{i,s}$, at the different pH values (Table 2) are within the same order of magnitude and are in good agreement with the binding constants obtained for the interaction of L in solution. The fit qualities of Langmuir and multivalency fits are identical, and therefore Figure 4 gives only the multivalency fits. These observations support the conclusions that (1) the binding motifs behave orthogonally at the CD SAM interface as well, (2) a considerable binding enhancement is observed at the surface leading to a preferential formation (expression) of CuL_2 via divalent binding at the interface at pH 6 although it is only a minor species in solution, and (3) the binding enhancement can be attributed solely to the effect of C_{eff}, and thus to multivalency, without the need for introducing cooperativity effects. The latter conclusion is in agreement with the homotropic systems discussed before.[4]

Multivalent enhancement at the CD surface is evident from a detailed analysis of the different species present in solution and at the surface at the different pH values. These results were obtained from the fitted SPR curves. Figure 5 depicts the results obtained for the concentration of the different species present at the CD surface. Concentrations of the species in solution are represented in the speciation (Figure 2).

The surface multivalency enhancement can be expressed by an enhancement factor, *EF*, which is defined as the ratio of the divalent ($[L]_{s,div}$) to monovalent ($[L]_{s,mono}$) concentrations of L at the surface divided by the analogous concentration ratio in solution ($[L]_{l,div}/[L]_{l,mono}$), according to eq 20.

$$EF = \left(\frac{[L]_{s,div}}{[L]_{s,mono}}\right) / \left(\frac{[L]_{l,div}}{[L]_{l,mono}}\right) = \frac{[L]_{s,div}{\cdot}[L]_{l,mono}}{[L]_{s,mono}{\cdot}[L]_{l,div}} \quad (20)$$

At pH 6, *EF* was larger than 200 at low coverages and gradually decreased at higher coverages.

To increase our understanding of heterotropic multivalency at the CD surface, we also prepared a metal complex using Ni(II) as the metal ion. This divalent cation with a coordination number of six forms complexes with an octahedral geometry. Ethylenediamine (en), for example, is known to give a trivalent $Ni(en)_3$ complex.[27] All solution species of L resulting from protonation and metal and CD_l complexation are given in the Supporting Information.

Similar to the case of Cu(II), when full orthogonality is assumed, all intrinsic stability constants for CD_l complexation of any species of L are equal. The divalent NiL_2 is expected to show the surface equilibria similar to CuL_2 given in Scheme 2, whereas the surface equilibria for the trivalent NiL_3 are given in the Supporting Information. A priori, $ML_3(CD_s)_3$ is expected as the major surface species for ML_3 because of the high effective concentration at the CD SAM.

The metal complex was prepared by mixing a solution of $NiCl_2$ and L in a 1:3 molar ratio. A geometric analysis of the most extended configuration of NiL_3 derived from CPK models (taking into account the two possible structural isomers) showed that the three adamantyl moieties are separated by about 3.0 nm. Considering the CD lattice periodicity of 2.1 nm, it is sterically feasible that all three adamantyl groups in the NiL_3 complex can interact with the CD SAM.

The protonation[25] and metal complex formation[26] constants corresponding to *N*-*n*-butylethylenediamine were used for the Ni(II) system as well. Similar to the Cu(II) complexes, the additional substitution at the en moiety with *N*-alkyl groups strongly reduces the metal complex formation constants.[26] These values lead to an expected pH dependence of the speciation of L in the presence of Ni(II) as shown in Figure 6.

The speciation diagram in the absence of Ni(II) is identical to the one described before (Figure 2, left). However, the trivalent NiL_3 is hardly expected (less than 5% at pH 11). This effect is due to K_{ML3} which is relatively small compared to K_{ML} and K_{ML2}, in particular for substituted en derivatives (such as *N*-*n*-butylethylendiamine) compared to en.[26]

SPR titrations were performed at pH 9 (1 mM $NaHCO_3$ and 1 mM CD_l) to ensure the maximum coordination number. SPR curves were fitted to the heterotropic multivalency model previously described. Analogous to the thermodynamic model for the Cu(II) complex, $K_{i,s}$ and the I_{max} were variables, while $K_{i,l}$ (6.0×10^4 M^{-1}) and C_{eff} (0.2 M) were fixed.

(30) Huskens, J.; Van Bekkum, H.; Peters, J. A. *Comput. Chem.* **1995**, *19*, 409−416.

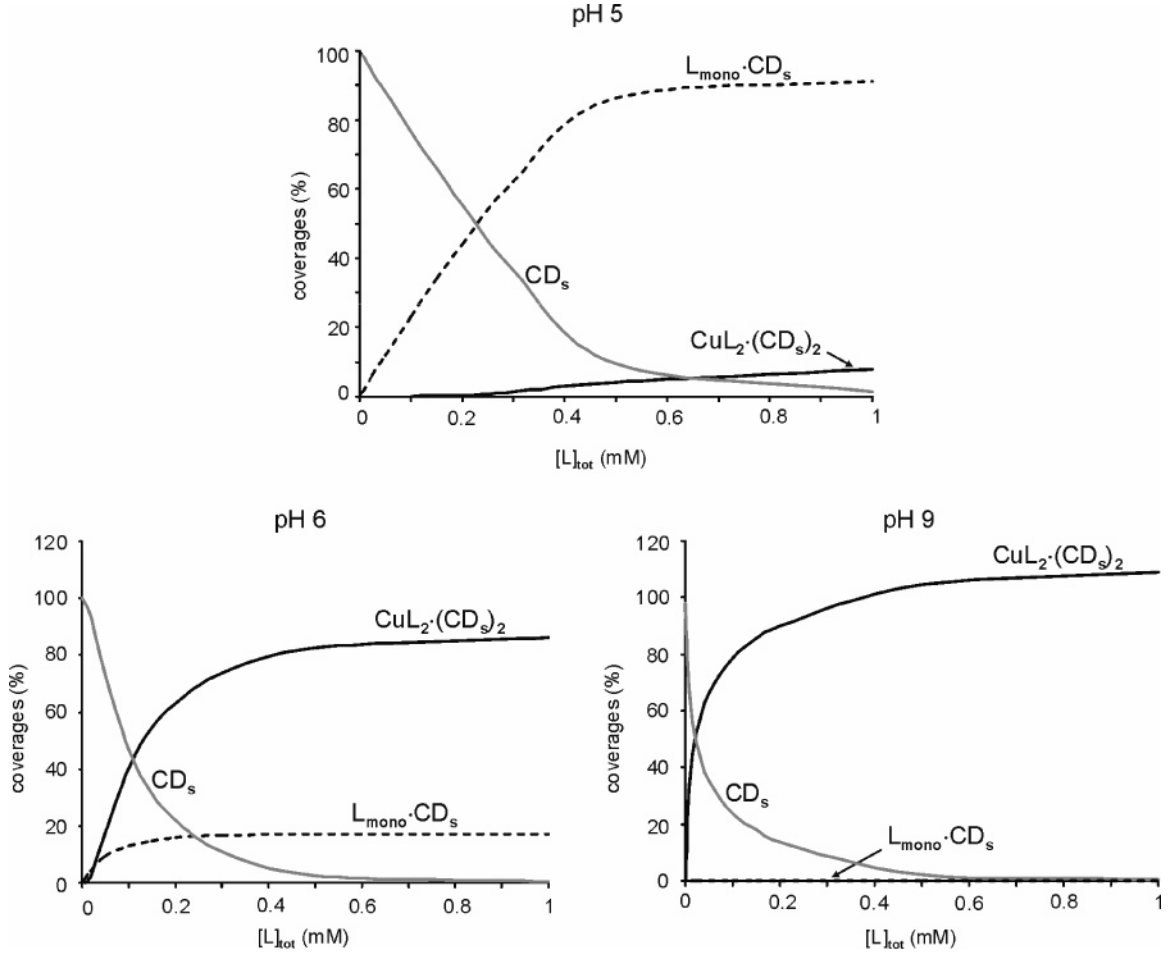

Figure 5. Surface coverages of monovalently bound L, L_{mono} (sum of concentrations of adsorbed H_2L, HL, L, CuL, and monovalently bound CuL_2) (dashed lines), the divalently bound CuL_2 (black solid lines), and uncomplexed CD_s present at a CD SAM at different pH's as a function of L_{tot} (with $Cu(II)_{tot}$:L_{tot} = 1:2).

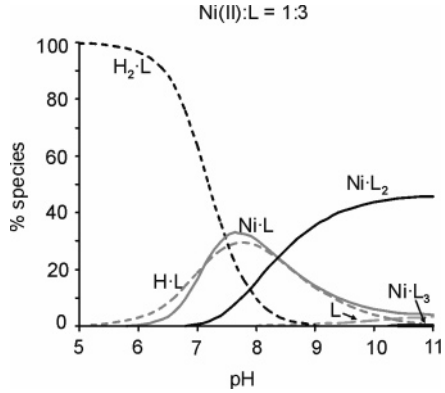

Figure 6. Speciation of L present in solution as a function of pH in the presence of Ni(II) (total concentration of L: 1 mM). Solid lines represent Ni(II) complexes and dashed lines represent species without Ni(II).

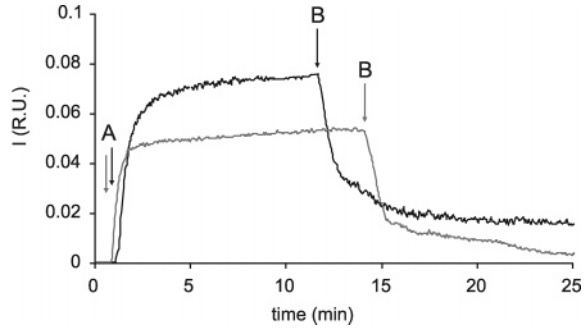

Figure 7. SPR time traces for the adsorption and desorption of of Ni^{2+}:L (black; $[Ni^{2+}]_{tot}$ = 0.5 mM; $[L]_{tot}$ = 1.5 mM) or Cu^{2+}:L (gray; $[Cu^{2+}]_{tot}$ = 0.5 mM; $[L]_{tot}$ = 1.0 mM) in a buffer of 1 mM 19 Na_2CO_3 (pH 11) and 5 mM CDl at CD SAMs; arrows indicate switching the flow solutions from buffer to M:L solution (A; onset of adsorption) and vice versa (B; onset of desorption).

The results obtained by fitting the SPR curves to a trivalent model gave a $K_{i,s}$ (3.4×10^4 M^{-1}) corresponding to an intrinsic adamantyl-cyclodextrin interaction[28] similar to the results obtained in solution. However, fitting the same SPR curve to a divalent model assuming that two adamantyls bind the CD surface gave an intrinsic binding constant, $K_{i,s}$, (3.4×10^4 M^{-1}), equal to the binding constant found when all three guest moieties are used in the complexation to the surface. Finally, fitting assuming monovalent binding gave a binding constant (5.7×10^5 M^{-1}) that is much higher than the K obtained in solution for an adamantyl-cyclodextrin interaction.[28] These results established that the binding is multivalent but that the thermodynamic model could not discriminate between trivalent and divalent binding.

To determine whether the Ni(II) complex adsorbing to the CD SAM is divalent or trivalent, desorption experiments were performed. Although the kinetics of adsorption and desorption are bound to be convoluted by mass transport limitation, a

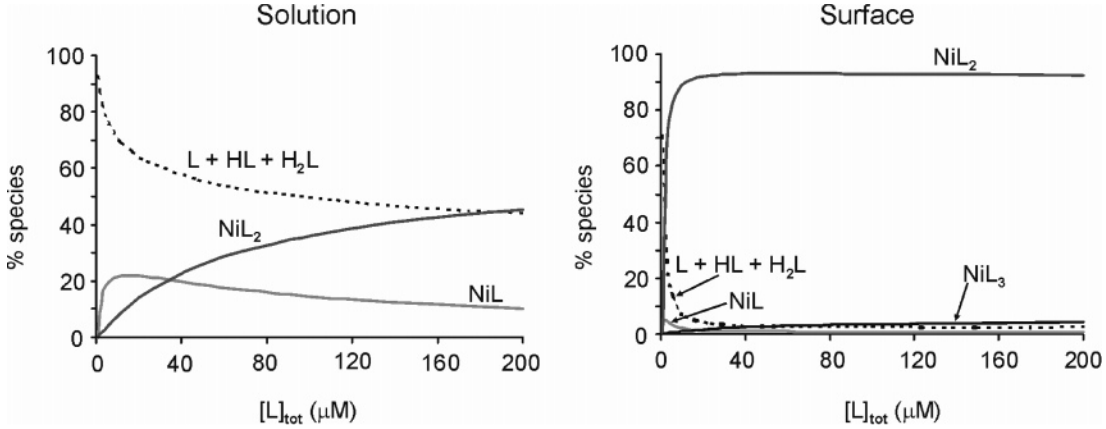

Figure 8. Concentrations of uncomplexed L (L, HL, H_2L) (dashed lines), NiL (solid line, light gray), NiL_2 (solid line, gray), and NiL_3 (solid lines, black) present in solution (left) and at the CD SAM (right) at pH 9 (1 mM $NaHCO_3$, 1 mM CDl) employing the sequential binding model for trivalent interactions.

difference is to be expected in particular in the desorption part of the SPR time traces when a difference in valency occurs.[5] SPR titrations were performed in the presence of 1 mM Na_2CO_3 buffer (pH 11) and 5 mM CD. Addition of a solution of Ni^{2+}:L ($[Ni^{2+}]_{tot}$ = 0.5 mM; $[L]_{tot}$ = 1.5 mM) or Cu^{2+}:L ($[Cu^{2+}]_{tot}$ = 0.5 mM; $[L]_{tot}$ = 1.0 mM), respectively, to the CD SAM resulted in an increase of the SPR signal, which leveled off after 10 min (see Figure 7). Rinsing of the surface with 1 mM Na_2CO_3 buffer (pH 11) and 5 mM CD was monitored for 30 min, until all guests had been completely removed. Similar desorption kinetics were observed for the Ni(II) and Cu(II) complexes (Figure 7). Since divalent binding was determined for the Cu(II) complex, the desorption experiments indicate also divalent binding for the Ni(II) complex, since multivalency is known to have a strong kinetic effect and a trivalent complex would desorb much slower than a divalent complex.[5,6c]

To find a possible explanation for the apparent divalency of the Ni(II) complex, the concentrations of the different species, $[L]_{free}$, [NiL], $[NiL_2]$, and $[NiL_3]$, were analyzed by using the sequential binding model with three interactions to the CD surface. Figure 8 shows the different species that are present in solution and at the CD surface at pH 9 and 1 mM CD_l concentration.

In contrast to the solution case, NiL_2 is essentially the only species at the surface, reaching complete coverage even at very low Ni^{2+} concentrations. At the surface, the trivalent NiL_3 reached up to 5%, but this is too low to be detected experimentally. Thus, a surface enhancement of the divalent NiL_2 is observed with an *EF* of ~100. The divalent species NiL_2, which is in minority in solution, is dominant at the surface. On the other hand, the monovalent species (L, HL, H_2L) and NiL, which are dominant in solution, are nonexistent at the surface. The *EF* for the trivalent NiL_3 is expected by the model to be about 10^4, but this is apparently still not enough to make it verifiable experimentally.

Conclusions

The binding of a host−guest metal−ligand complex formed between an adamantyl-functionalized ethylenediamine (L) and an M(II) ion at CD SAMs resulted from multivalency of the guest molecules. At pH 6, the multivalent surface clearly enhanced the presence of the divalent CuL_2 complex at its interface, whereas the monovalent CuL was the majority species in solution. This behavior is attributed to the high C_{eff} of cyclodextrin sites present at the surface and the close-to-optimal linker lengths between the two adamantyl groups relative to the periodicity of the CD lattice (ca. 2 nm).[22] The Ni(II) complex was studied at pH 9 and was compared to the Cu(II) complex. The sequential multivalent, heterotropic binding model, although successful in explaining the divalent binding of the CuL_2 complex, could not discriminate between two or three interactions for the Ni(II) system. Desorption experiments showed a similar behavior for both the Ni(II) and Cu(II) complexes, which is an indication of divalent binding for both complexes.

In conclusion, we have shown a new concept of surface-enhanced expression of multivalent species at interfaces using two types of orthogonal noncovalent interactions (host−guest and metal−ligand coordination). We believe that this surface enhancement can be used in nanofabrication schemes targeted at the formation of large molecular assemblies driven by multivalent interactions.

Experimental Section

Materials. Chemicals were obtained from commercial sources and were used as such. β-Cyclodextrin (CD) was dried in vacuum at 80 °C in the presence of P_2O_5 for at least 5 h before use. Solvents were purified according to standard laboratory methods. Millipore water with a resistivity larger than 18 MΩ·cm was used in all our experiments. Synthesis of the CD heptathioether adsorbate was reported previously.[20] NMR spectra were recorded on Varian AC300 and AMX400 spectrometers. FAB-MS spectra were recorded with a Finnigan MAT 90 spectrometer using *m*-nitrobenzylalcohol as the matrix.

***N*-[2-(2-{2-[2-(Adamantan-1-yloxy)ethoxy]ethoxy}ethoxy)-ethyl]ethane-1,2-diamine (L).** A stirred solution of triethylene glycol bromoethyl adamantyl ether[31] (0.65 g, 1.6 mmol) in an excess of ethylenediamine (20 mL) was heated to 80 °C overnight under a nitrogen atmosphere. The reaction mixture was cooled down to room temperature and was evaporated under reduced pressure. The crude product was separated by flash column chromatography (CH_2Cl_2:EtOH:NH_4OH, 1:1:0.1−1:4:0.4, v/v) to afford the compound as a yellow oil (0.58 g, 93%).

(31) Mulder, A.; Onclin, S.; Péter, M.; Hoogenboom, J. P.; Beijleveld, H.; Ter Maat, J.; García-Parajó, M. F.; Ravoo, B. J.; Huskens, J.; Van Hulst, N. F.; Reinhoudt, D. N. *Small* **2005**, *1*, 242−253.

^{1}H NMR (300 MHz, $CDCl_3$): δ (ppm) 3.67−3.58 (m, 12H, AdOCH_2 and (CH_2OCH_2)$_3$), 2.81 (t, J = 5.7 Hz, 2H, CH_2CH_2-NH), 2.80 (t, J = 5.3 Hz, 2H, NHCH_2CH_2), 2.70 (t, J = 5.4 Hz, 2H, $CH_2CH_2NH_2$), 2.13 (m, 3H, CH_2CHCH_2[Ad]), 1.96 (m, 6H, CHCH_2C[Ad]), 1.73−1.74 (m, 6H, CHCH_2CH[Ad]); ^{13}C NMR (75 MHz, $CDCl_3$): δ (ppm) 72.4, 71.5, 70.8−70.5, 59.5, 52.3, 49.2, 41.7, 36.7, 30.7. MS (MALDI-TOF): *m/z* calcd for $C_{20}H_{38}N_2O_4$ 370.2; found 371.1 $[M + H]^+$; elemental analysis: H 10.34, C 64.83, N 7.56, calcd for $C_{20}H_{38}N_2O_4$; found: H 10.38, C 62.87, N 7.07.

Preparation of the Metal Complex Form of L with Cu(II) and Ni(II). The metal complexes of Cu(II) and Ni(II) with L were prepared by mixing aliquots of a concentrated solution of $CuCl_2$ and $NiCl_2$ in distilled water (Millipore) to a solution of L. The molar ratio of metal and L was maintained at exactly 1:2 (Cu(II)) and 1:3 (Ni(II)) to prevent the formation of metal hydroxides. After addition of the metal salts, the solutions were brought to the corresponding buffer solution (1 mM) and the CD concentration (1 mM).

Substrate and Monolayer Preparation. All glassware used to prepare monolayers was immersed in piraña (conc. H_2SO_4 and 33% H_2O_2 in a 3:1 ratio). (Warning! piraña should be handled with caution; it has detonated unexpectedly.) The glassware was rinsed with large amounts of high-purity water (Millipore). All solvents used in monolayer preparation were of p.a. grade. All adsorbate solutions were prepared freshly prior to use. Round glass-supported gold substrates for SPR (2.54 cm diameter; 47.5 nm Au) were obtained from Ssens BV (Hengelo, The Netherlands). Gold substrates were cleaned by immersing the substrates in piraña for 5 s and leaving the substrates for 5 min in absolute EtOH.[32] The substrates were subsequently immersed into a 0.1 mM CD heptathioether adsorbate solution in EtOH and $CHCl_3$ (1:2 v/v) for 16 h at 60 °C. SAMs of 11-mercaptoundecanol were adsorbed from EtOH at room temperature for 24 h. The samples were removed from the solution and were rinsed with substantial amounts of chloroform, ethanol, and Millipore water.

Calorimetric Titrations. Calorimetric measurements were performed at 25 °C using a Microcal VP-ITC instrument with a cell volume of 1.4115 mL. Sample solutions were prepared in Millipore water. For studying the complexation of L to native CD at different pH's (2, 7, 9, 11), 5-μL aliquots of a 5 mM solution of L were added to a 0.5 mM solution of CD in the calorimetric cell, monitoring the heat effect after each addition. For studying the complexation of L in the presence of Cu(II) (Cu(II):L = 1:2) to CD at different pH's (7, 9), 5-μL aliquots of a 10 mM solution of CD were added to a solution of 0.5 mM $CuCl_2$ and 1 mM L. Dilution experiments showed that at the experimental concentrations employed in these experiments, none of the three species showed any detectable aggregation in water.

Surface Plasmon Resonance (SPR) Sspectroscopy. The SPR setup was obtained from Resonant Probes GmbH.[33] A light beam from the HeNe laser (JDS Uniphase, 10 mW, λ = 632.8 nm) passes through a chopper that is connected to a lock-in amplifier (EG&G, 7256). The modulated beam then passes through two polarizers (Owis), by which the intensity and the plane of polarization of the laser can be adjusted. The modulated beam passes a beam-expanding unit (spatial filter) with a pinhole (25 μm) for spectral cleaning of the wave fronts. The light is coupled via a high index prism (Scott, LaSFN9) in this Kretschmann configuration to the (Au) metal-coated substrate which is index-matched to the prism in contact with a Teflon cell having O-rings for a liquid-tight seal. The sample cell is mounted on top of a $\theta-2\theta$ goniometer with the detector measuring the reflectivity changes as a function of the angle of incidence of the p-polarized incoming laser beam. The incoming s/p laser beam passes through a beam splitter, which splits the p- and the s-polarized light. The s-polarized light is conducted to a reference detector. The p-polarized light passes a beam-expanding unit (spatial filter) with a pinhole (25 μm) for spectral cleaning and control of the intensity of p-polarized light and is collected into a photodiode detector. Titrations were measured in real time by recording the changes in the reflectivity in the fixed angle mode (55.2°). Titrations were performed starting with a buffer solution in the cell which was replaced by increasing concentrations of the analyte (L in the absence and presence of Cu(II) (Cu(II):L = 1:2). After addition of the analyte and stabilization of the SPR signal, the cell was thoroughly rinsed with 10 mM CD (in the corresponding buffer) followed by rinsing with buffer solution. The same procedure was repeated until complete restoration of the CD surface. SPR measurements were performed under continuous flow using a peristaltic pump at 0.5 mL/min. Reflectivity changes due to solution concentrations were found to be negligible under the present conditions.

Modeling. The thermodynamic model was implemented in Excel (Microsoft Excel 2000), as described before.[5] For a more detailed description and the equations corresponding to the equilibrium constants and the mass balances, see the main text. For the Cu−L system, the following parameters were used: $K_{HL} = 2.00 \times 10^{10}$ M^{-1},[25] $K_{HL2} = 3.39 \times 10^7$ M^{-1},[25] $K_{CuL} = 8.71 \times 10^9$ M^{-1},[26] $K_{CuL2} = 1.89 \times 10^8$ M^{-1},[26] $K_{i,l} = 6.0 \times 10^4$ M^{-1} (see above), and $C_{eff,max} = 0.20$ M. For the Ni−L system, the following parameters were additionally used: $K_{NiL} = 5.37 \times 10^6$ M^{-1}, $K_{NiL2} = 3.63 \times 10^5$ M^{-1}, and $K_{NiL3} = 1.58 \times 10^2$ M^{-1}.[26] In the fitting procedure, all protonation, metal−ligand complexation, and solution Ad−CD complexation constants were kept constant, while the surface Ad−CD interaction was varied as a fitting parameter.

Acknowledgment. We are grateful for financial support by the Council for Chemical Sciences of The Netherlands Organization for Scientific Research (NWO-CW) in the Young Chemists programme (O. C. B.; grant 700.50.522 to J. H.).

Supporting Information Available: Speciation schemes for the solution and surface equilibria of the Ni−L system. This material is available free of charge via the Internet at http://pubs.acs.org.

JA0637705

(32) Ron, H.; Rubinstein, I. *Langmuir* **1994**, *10*, 4566−4573.
(33) Aust, E. F.; Ito, S.; Sawondny, M.; Knoll, W. *Trends Polym. Sci.* **1994**, *2*, 313−323.